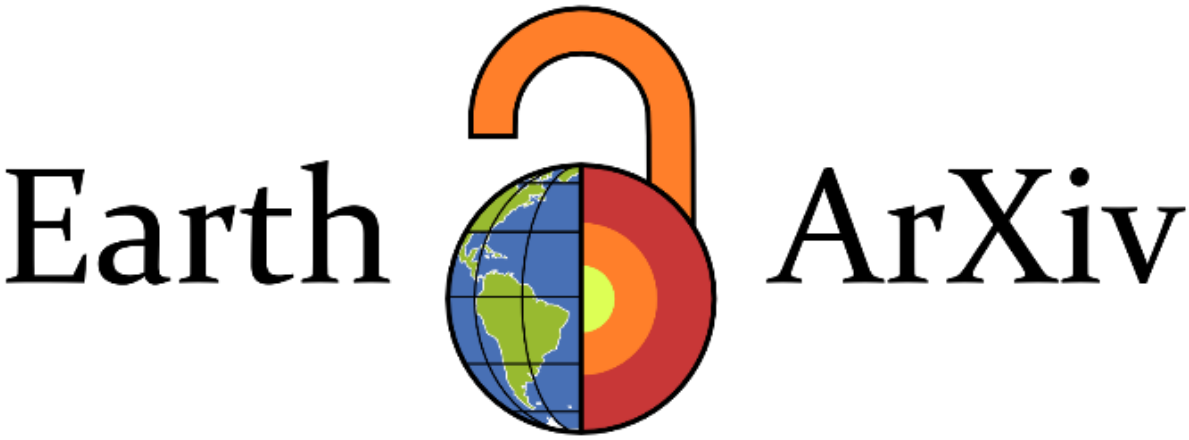

Injecting vegetation-based spatialization in the hydrogeological framework for erosion modelling

Marianna Miola, Ulderico Fugacci

Istituto di Matematica Applicata e Tecnologie Informatiche
del Consiglio Nazionale delle Ricerche (CNR-IMATI)
Via de Marini 6, 16140, Genova, Italy

marianna.miola@cnr.it, ulderico.fugacci@cnr.it

Abstract

Erosion processes and landslide are widespread across Italy and frequently cause significant damage to people, infrastructure, and ecosystems. These processes are primarily triggered by rainfall events, whose impact depends on multiple interacting factors, including geomorphology, soil properties, land use, and vegetation. Among these, vegetation plays an essential role in regulating hillslope hydrology by controlling interception, infiltration, and runoff. However, current hydrogeomorphological modelling framework lacks systematic methods to incorporate vegetation variability at the sub-grid scale, typically relying on coarse land cover (LC) classification and simplified class-based parametrization.

This work presents a computational framework to explicitly incorporate sub-grid vegetation variability into soil erosion modelling, with a focus on its impact on Curve Number (CN) estimation for runoff and potential erosion assessment. Vegetation is represented as a spatially distributed categorical variable and modelled through an indicator-based geostatistical approach, allowing the propagation of spatial uncertainty into hydrological condition (h_c) evaluation and CN assessment.

The proposed approach integrates (1) a GIS-based pipeline for geospatial and watershed analysis, (2) a stochastic spatial model of vegetation based on point observations and structured mesh support, and (3) erosion modelling within a unified workflow. The methodology is designed to be transferable across different study areas and data availability conditions.

The entire approach is tested on a real case study in Monte Pisano (Tuscany, Italy), an area affected by wildfire in 2018. Prior to erosion modelling, the stochastic-based vegetation modelling is validated under different sampling configurations to assess robustness and sensitivity. Results show that the stochastic framework produces erosion

estimates broadly consistent with deterministic approaches, while enabling the explicit representation of sub-grid variability and associated uncertainty. Although a slight underestimation is observed, the probabilistic characterization enhances the interpretability of model outputs and supports more informed decision-making. By reducing reliance on subjectively defined parameters, as the hydrologic condition, adn embedding uncertainty into the modelling chain, the proposed framework represents a shift toward advancing environmental modelling practice, promising direction for further research in joining biodiversity and hydro-geomorphological applications.

1 Introduction

Vegetation is a primary factor regulating hillslope hydrology and geomorphological processes. Leaf canopies intercepts rainfall, reducing its kinetic energy, while root systems reinforce the soil and promote infiltration. The effectiveness of these mechanism varies with vegetation structure, composition and spatial coverage, making vegetation as a key control on geomorphological dynamics.

Recent research on vegetation-geomorphology interactions has revealed limitations in traditional approaches that treat these processes separately and unidirectionally [Mar10]. Instead, growing evidence supports the existence of strong bidirectional feedbacks between ecological and geomorphic systems. Linking these processes across spatio-temporal scales remains a central challenge in bio-geomorphology, and their integration into operational modelling frameworks is still largely unresolved [CPA+24]. Plant functional traits have been recognized as key mediators of vegetation–geomorphology interactions, as they directly influence hydrological and erosion processes, signalling the need for a more integrated research approach where geomorphology and ecology inform each other [Hau11].

These feedbacks are particularly relevant on disturbed hillslopes. After disturbance, pioneer species establish and, once they reach a critical size, initiate interactions between vegetation and hydro-geomorphological processes. This leads to the co-evolution of plant communities and landforms, which can be abruptly reset by events such as wildfires [Gur14, Vil20].

Despite this, vegetation dynamics are still poorly represented in operational hydrological models. This limitation is becoming increasingly critical under climate change, which is expected to intensify both extreme rainfall and wildfire disturbances, enhancing vegetation loss and slope instability [GG16].

A major limitation concerns how vegetation is managed. Vegetation strongly controls hydrological response, yet its spatial and temporal variability is rarely accounted for. The Soil Conservation Service – Curve Number (SCS-CN) method, which links land cover to surface runoff, is typically

assigned from lookup tables and relies on fixed values derived from land cover and soil classifications [usd21, MS03].Several studies have proposed modifications to account for vegetation characteristics and improve runoff prediction, for example by adjusting CN values for different vegetation types [HWWVM08, SVDL09, YCW$^+$25].

Vegetation is crucial to define the hydrologic condition (h_c), which represents the effect of vegetation density, structure, and management on runoff generation. However, h_c is commonly treated as a fixed categorical input, neglecting its sub-grid spatial variability. This simplification masks the heterogeneity that affects real hillslope behaviour [MS03].

In this work, our main contribution is to introduce a stochastic, spatially distributed representation of vegetation that replaces the conventional deterministic assignment based on land cover (LC) classes. The proposed approach integrates geostatistical modelling of vegetation into a hydro-geomorphological framework for erosion assessment by propagating the probability distribution of vegetation classes into the Curve Number (CN) estimation. In particular, stochastic vegetation maps are built on a regular grid support; combining all occurrence probabilities of vegetation classes is then used to modulate hydrological conditions (h_c), affecting CN assessment.This allows vegetation-related uncertainty to be explicitly propagated throughout the modelling chain, improving the representation of erosion processes across scales. The methodology is implemented through a computational workflow combining: (1) a GIS-based geospatial and watershed analysis, (2) a stochastic modelling of vegetation spatial distribution on high-resolution geometric mesh support (i.e., *Modeling Uncertainty as a Support for Environment* – `MUSE` tool [Mio25, MCPVZ22]), and (3) a coupled hydro-geomorphological model for erosion assessment (`LANDPLANER` [Ros14]).

The methodology is applied on a real case study in the site of Monte Pisano (Tuscany, Italy), an area severely affected by wildfire in autumn 2018. The approach produces erosion estimates consistent with the traditional deterministic method, while providing additional uncertainty-informed insights that enhance result interpretation and support more informed decision-making. By shifting from a deterministic to a stochastic paradigm in vegetation parametrization, this work highlights a novel and promising direction for improving hydro-geomorphological modelling.

The paper is organized as follows. Section 2 describes the background, including both the traditional hydro-geomorphological pipeline and the role of vegetation. Our methodology is presented in Section 3. Section 4 presents the case study reporting geological characterization, available data, and the application of the methodology. Results are presented in Section 5, respectively divided into validation of the stochastic vegetation modelling by employing classification metrics (i.e., overall accuracy and Cohen's Kappa coefficient) and the comparison of erosion estimates with and without spa-

tially distributed vegetation. Section 6 and Section 7 conclude the paper, outlines current limitations and future directions.

2 Background

In conventional approaches, erosion modelling relies on three main components: (1) geospatial and watershed analysis derived from a Digital Terrain Model (DTM), (2) estimation of surface runoff using the SCS-CN method, and (3) evaluation of erosion susceptibility based on hydrological and topographic information. Within this framework, vegetation affects runoff generation through the hydrologic condition (h_c), which is typically assigned deterministically from land cover classes.

Geospatial and watershed analysis The first component consists of a standard GIS-based topographic analysis, widely used in geomorphological and hydrological applications. Starting from a raster Digital Terrain Model (DTM), primary terrain attributes are computed, including slope, flow accumulation, and drainage network by watershed analysis. The latter is typically performed using the D8 single flow direction (SDF) algorithm [Ehl89], which assigns each cell a flow direction towards the steepest downslope neighbour, routing all accumulated flow to a single cell. The resulting topographic variables provide the morphological inputs for hydrological modelling and erosion assessment.

Hydrological framework and Curve Number estimation Surface runoff is estimated using the SCS Curve Number (CN) method [usd21], which relates rainfall to runoff as a function of land cover and soil properties. CN values are derived by combining land use/land cover (LULC) information with Hydrologic Soil Groups (HSG) through standard lookup tables.

LULC data are obtained from the Corine Land Cover (CLC) dataset, while HSG information describes soil infiltration capacity. In standard practice, each LULC–HSG combination is associated with a fixed CN value, typically assuming an average hydrologic condition (h_c), such as "fair", or a range of CN values, varying according to h_c conditions, in the case of missing specific information.

Erosion modelling For the erosion phenomena modelling, different methodology represents the state-of-the-art, such as based on topographic thresholds [TP14] or RUSLE approach [R$^+$91].

In this context, erosion is evaluated through a dual modelling scheme, implemented into `LANDPLANER` tool [Ros14]. The first component is an empirical topographic threshold approach that identifies cells prone to erosion

The entire hydro-geomorphological framework, including GIS analysis, CN evaluation and erosion modelling, is represented in the scheme in Figure 1.

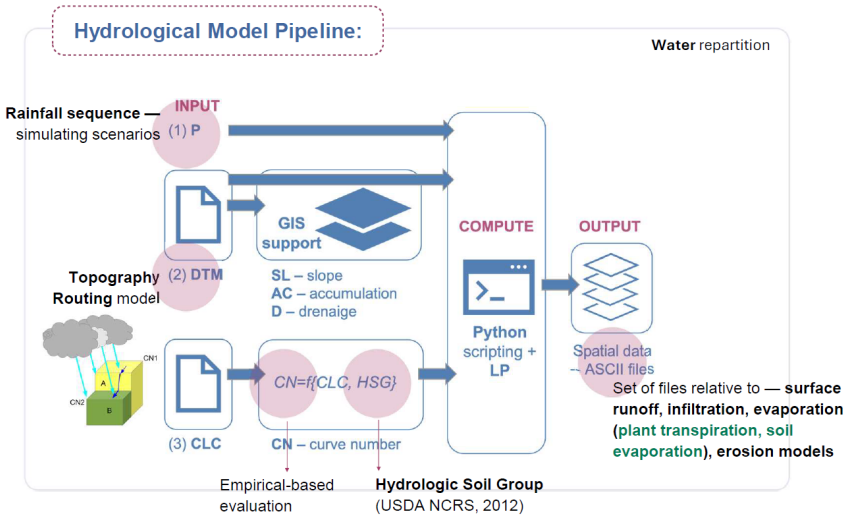

Figure 1: Hydrological model pipeline, involving GIS for geospatial data processing and erosion modelling by the third-party code `LANPLANER`.

initiation based on slope morphology, vegetation and land use. The second component is an erosion index derived from hydrological outputs, such as primarily surface runoff and infiltration; combining with the topographic threshold provides a map of erosion susceptibility.

The role of vegetation Within traditional hydro-geological framework, vegetation influences runoff generation through the hydrologic condition (h_c), which reflects canopy cover, vegetation density, and management practices. In standard implementations, h_c is assigned as a fixed categorical parameter associated with land cover classes [usd21].

However, widely used land cover datasets, such as the CORINE Land Cover (CLC) are characterized by relatively coarse spatial resolution and do not capture the fine-scale variability in vegetation patterns. As a result, h_c is assumed homogeneous within each class, neglecting sub-grid heterogeneity that can significantly influence runoff generation and erosion dynamics [VNN11].

In ecological and biodiversity studies, spatial statistical approaches are commonly employed to model species distribution and habitat suitability. These applications are often based on regression-based species distribution models or machine learning techniques [EL09, Fra45] rather that geostatistical simulation of mutually exclusive categorical classes.

In contrast, soil erosion modelling frameworks typically rely on deterministic land cover maps derived from remote sensing products, where vege-

tation classes are treated as fixed spatial inputs [WS78, Ren97]. The spatial uncertainty and short-range heterogeneity of vegetation patterns are rarely propagated into erosion simulations. Consequently, the potential impact of categorical spatial variability on erosion estimates remains insufficiently explored.

At the state of the art, several correction strategies have been proposed to improve the classical Curve Number method, such as regression-based CN recalibration, incorporating of soil and hydraulic parameters, dynamic adjustment for vegetation phenology, hybrid CN–infiltration models, and satellite- or NDVI-based CN corrections [WZS$^+$25, MHHJ19, AMTR22, GU04]. These approaches remain largely deterministic and spatially coarse.

The present work addresses vegetation-based CN correction by introducing a stochastic, spatially distributed representation of vegetation, explicitly propagating class probabilities through the Curve Number framework to better capture the effects of vegetation heterogeneity on runoff and erosion.

3 Modelling framework

The proposed framework builds upon a standard hydro-geomorphological modelling pipeline for erosion evaluation and extends it by explicitly accounting for vegetation spatial variability. It is represented in Figure 2.

In particular, we introduce a geostatistical approach to explicitly model the spatial variability of vegetation classes at finer scales. This allows the reconstruction of spatially structured patterns within land cover classes and provides a basis for deriving a spatially variable and probabilistic representation of h_c, which is then propagated into the estimation of the Curve Number and, ultimately, into erosion modelling.

Stochastic methods, based on geostatistics, are widely used in geosciences to reconstruct heterogeneous spatial patterns from sparse observation [G$^+$97]. In this work, vegetation classes are managed as a set of mutually exclusive categories and encoded as indicator (Equation (1)), whose spatial distribution is estimated by using an stochastic simulation approach.

$$i(\mathbf{u}_\alpha; s_k) = \begin{cases} 1 & \text{if } s(\mathbf{u}_\alpha) = s_k \\ 0 & \text{otherwise} \end{cases} \qquad k = 1, \ldots, K \tag{1}$$

$$\gamma_I(\mathbf{h}; s_k) = \frac{1}{2N(\mathbf{h})} \sum_{i=1}^{N(\mathbf{h})} [i(\mathbf{u}_\alpha; s_k) - i(\mathbf{u}_\alpha + \mathbf{h}; s_k)]^2 \tag{2}$$

Basically, the variography is composed of two main step, such as (1) the experimental points calculation and (2) searching the best fitting model (among a set of positive-definite permissible ones) of points. Representative parameters of the best-fit model are indices of the existing spatial cor-

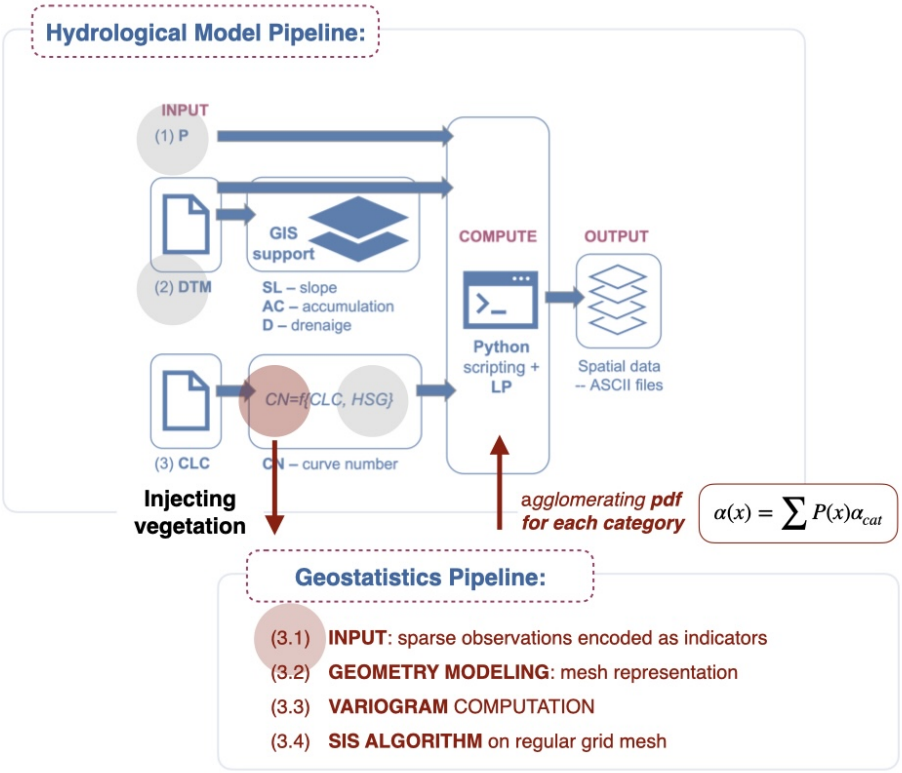

Figure 2: Our proposed framework: injecting vegetation by geostatistics in the traditional hydro-geomorphological modelling framework.

relations (range and sill parameters) between samples and the short-scale variability (nugget effect).

After evaluating the existence of spatial dependence laws (indicator variogram; see Equation (2)), Sequential Indicator Simulation (SIS) is applied to estimate indicator values in unsampled locations of the target area, consistent with both the observed data and their spatial correlation. At each simulation iteration, the algorithm uses the Indicator Kriging, to estimate the local probability of occurrence for each category, building a discrete conditional probability distribution.

Combining SIS realisations is used in the subsequent step to derive a probabilistic representation of the Curve Number (CN), providing the link between the geostatistical and geomorphological components of the framework.

4 The case study

4.1 The study area

The Monte Pisano site is located in northern Tuscany (central Italy), positioned at the watershed between the Pisa and Lucca plains and bounded by the Arno and Serchio rivers. It is part of the Tuscan Sub-Apennine chain, extending from the Apuan Alps, with elevations up to approximately 900 m a.s.l (i.e., Monte Serra, 918 m a.s.l.) [RT74, Del87, CCCP13].

The area is geologically part of the metamorphic Tuscan units, dominated by quartzites and phyllites, and features steep hillslopes with narrow valleys and ephemeral streams, making it highly susceptible to surface erosion and shallow landslides. The climate is Mediterranean and and vegetation forms a disturbance-driven mosaic, with sclerophyllous communities (e.g., *Quercus ilex*) prevailing at lower elevations, and chestnut (*Castanea sativa*) stands and mixed forests at higher altitudes. Pine forests (*Pinus pinaster*), largely of secondary origin, are widespread and reflect past land use and recurrent fire [BST$^+$04].

In September 2018, a severe wildfire burned ≈1,100 hectares of forest and terraces, spreading on areas of Calci, Vicopisano, and Buti (Province of Pisa, Tuscany, Italy). A second fire event affected more than 200 hectares of pine forest of the area of Vicopisano in February 2019. The fire affected different vegetation types with contrasting severity and geomorphic impacts, drastically reducing protective cover, altering soil properties, and creating hydrophobic layers.

4.2 Available data

The geospatial dataset used in this study are provided by "Regione Toscana – Open Data (dati.toscana.it)" It includes:

- a high-resolution Digital Terrain Model (DTM) with a resolution of 10×10 meters;
- CORINE Land Cover maps (1:10000), period 2007-2019, covering all the regional area and contains LULC classes according to the CORINE Land Cover classification (III-IV level);
- pedological database for soil features (hydrologic soil group, HSG).

Additionally, a pre-fire events vegetation map (August, 2018) is used as observational basis for the spatial modelling of vegetation. The map is derived from [BST$^+$04], integrating surveys of spring 2018. Such processing is published in a technical document for the realization of restoration measures for forested areas affected by the 2018, Calci and 2019, Vicopisano wildfires [SFAB20], approved by Regione Toscana by *Decreto dirigenziale* n°2420 of 20/02/2020.

Transition type	area (ha)	
Other (unchanged)	1,407 ha	(39.7%)
Vegetation (unchanged)	1,348 ha	(38.0%)
Vegetation → Burned	780 ha	(22.0%)
Other → Other	6 ha	(0.2%)
Vegetation → Other	2 ha	(0.0%)

Table 1: Land cover change summary, detecting the transition type (e.g., from vegetation to burned area or unchanged areas) and the coverage area (in ha and %). The latter is computed for each detected transition and expressed as a percentage on the total area.

All data are related to the Project "National Biodiversity Future Center - NBFC".

4.3 Hydrologic modelling

Standard GIS preprocessing has been firstly applied to derive catchment boundaries, flow networks, and topographic outputs. Results are represented in the Figure 3, showing respectively the (a) Digital Terrain Model, (b) slope, (c) drainage direction, and (d) flow accumulation maps, with a resolution of 10×10 meters.

As previously described, the Curve Number (CN) map represents the core hydrological input for erosion modelling. CN values are derived by combining land cover information (from Corine Land Cover datasets; see Figure 4) with soil properties (Hydrologic Soil Groups, HSG), using established lookup tables, and the hydrologic condition (h_c), ranging from *good*, *fair*, and *poor*.

Figure 5(a) shows the map of detecting vegetation in CLC2016, used to evaluate land cover changes after fire event in the 2018. Figure 5(b) represents the land cover changes in the period 2016-2019, highlighting a clear fire-driven reorganization of the landscape. Most changes correspond to transitions from natural vegetation to burned areas (i.e., red areas), indicating that forests and semi-natural ecosystems were primarily affected. Although post-fire recovery is observed, it remains limited compared to vegetation loss, suggesting that regeneration processes are still ongoing in the 2019 and spatially heterogeneous. Table 1 quantifies the differences induced by fire-event comparing CLC106-2019 in terms of area (in ha and %).

While LULC information is derived from the Corine Land Cover dataset, the HSG (from pedological database) presents local inconsistencies and missing values that we have explicitly addressed by rules. First, when land cover information is available at a level coarser than CLC Level III, CN values are assigned by aggregating lookup table entries from finer classes. Specifically, values are upscaled to Level II or Level I by averaging the corresponding

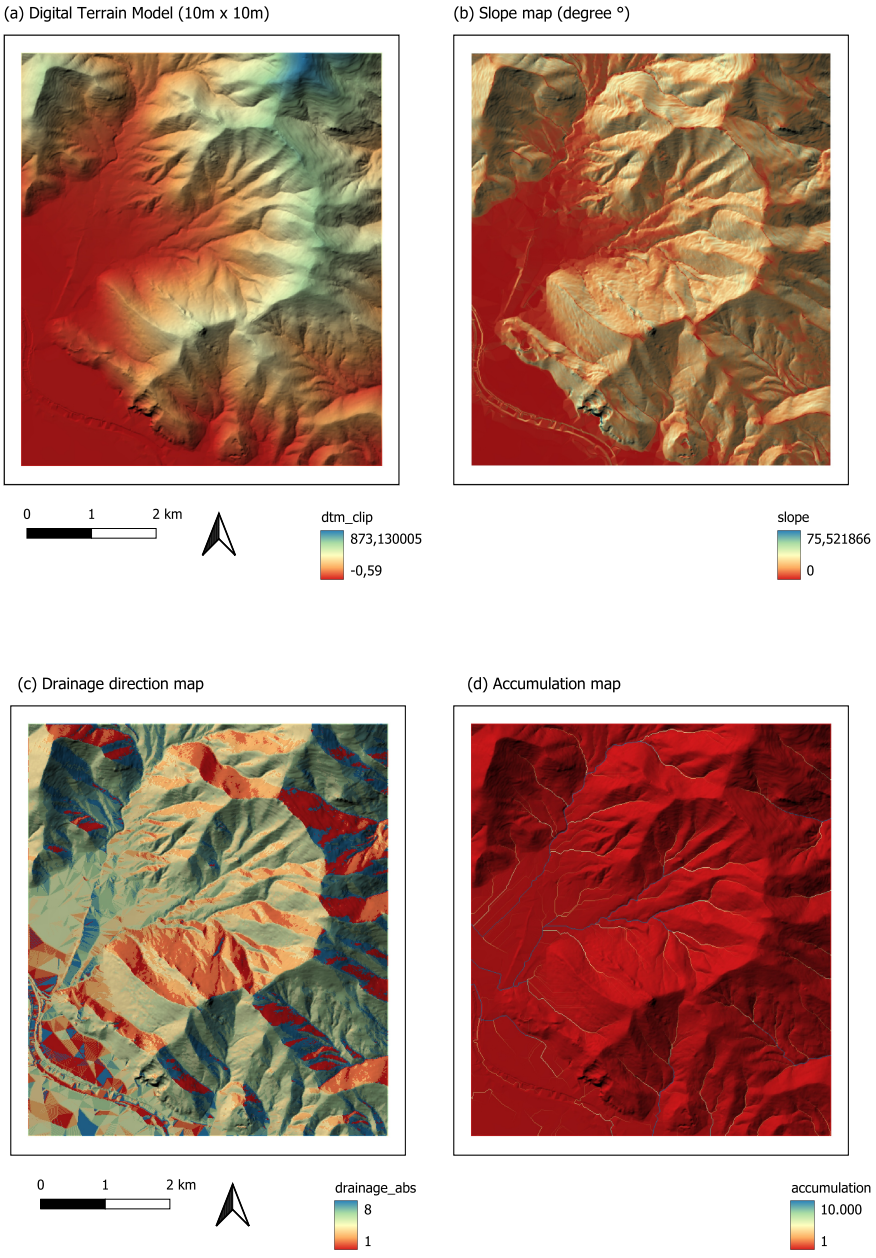

Figure 3: Geospatial analysis of Monte Pisano site: (a) Digital Terrain Model with a original resolution of 10×10 m, (b) slope, (c) drainage direction and (d) accumulation maps.

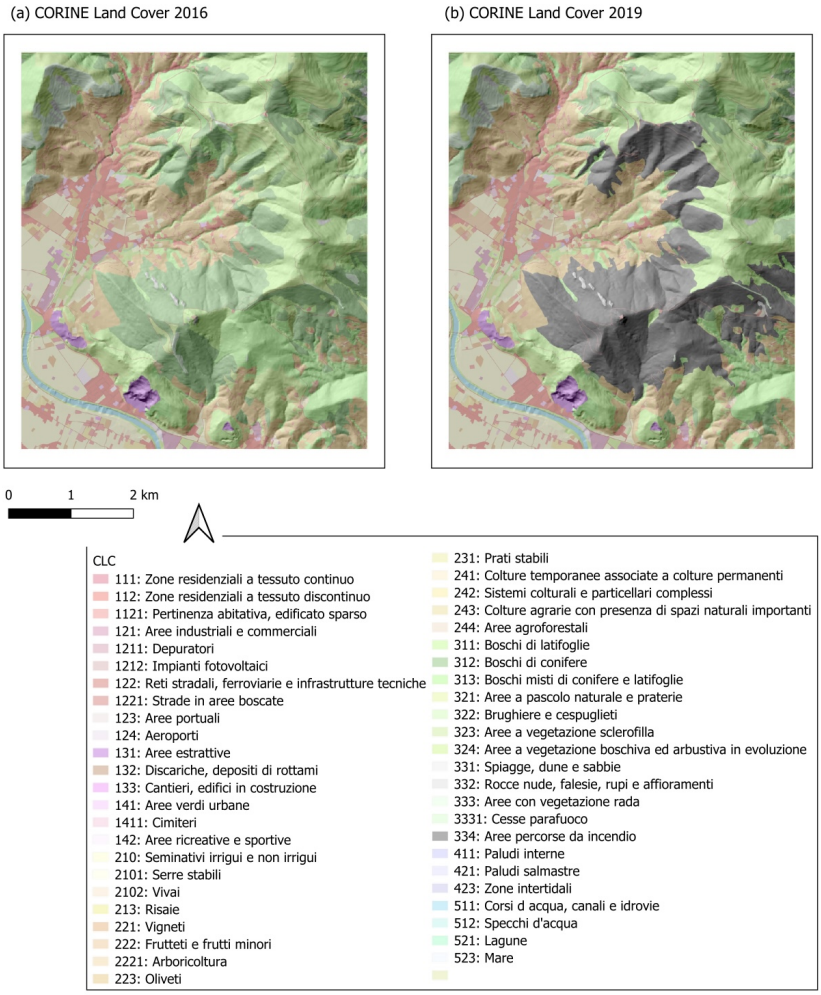

Figure 4: CORINE Land Cover maps for the year 2016 and 2019, clipped to the target area.

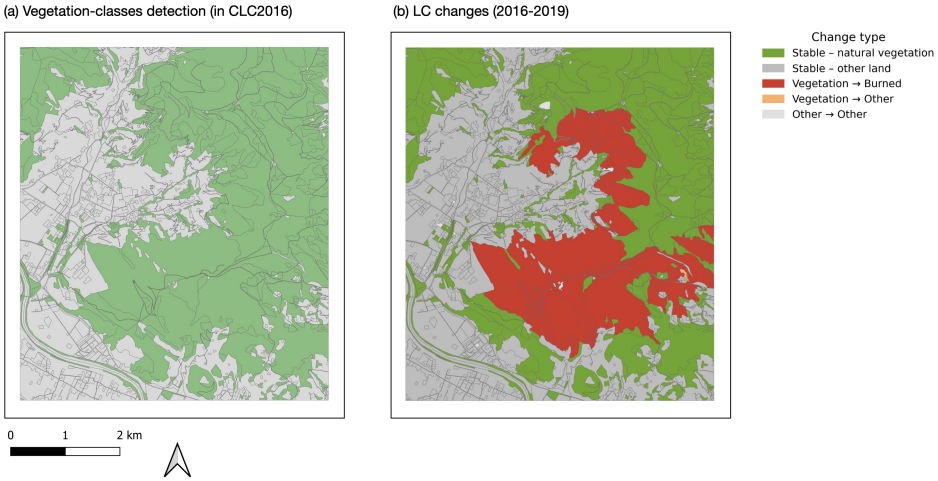

Figure 5: CLC2016-2019: differences map pre- and post- fire event.

CN values, ensuring consistency across classification levels. Second, in cases where HSG information is missing, different strategies are adopted depending on land cover type. For urban surfaces (CLC class 1), a fixed CN value representative of low infiltration capacity is assigned. For all other cases, missing HSG values are reconstructed using a spatial proximity assumption. Specifically, a centroid-based nearest-neighbour procedure is implemented in a GIS environment. Polygons lacking HSG information are matched to the closest polygon with a valid HSG value, based on centroid distance.

Each LULC-HSG combination links to a set of corresponding CN values (i.e., minimum, mean, and maximum CN). Figure 6 shows the CN maps, ranging from minimum, mean and maximum values, obtained from each combination of CLC2016-HSG in the study area.

After inputs preparation, the erosion modelling is perfomed in LANDPLANER [Ros14]. For all simulated scenarios, the hydrological framework results into the erosion estimation on a pixel-based model of 10×10 meters (according to the original DTM resolution). Specifically, we visualize the erosion maps for different synthetic rainfall scenarios, ranging from 20 mm to 140 mm, with an increment of 20 mm.

Figure 7 and Figure 8 shows the results of simulations in terms of erosion index varying synthetic rainfall scenarios and considering CN map derived from CLC2016 (pre-fire event) and CLC2019 (post-fire event), respectively. Figure 9 compares pre- and post-fire results as erosion maps computed with minimum, average and maximum CN.

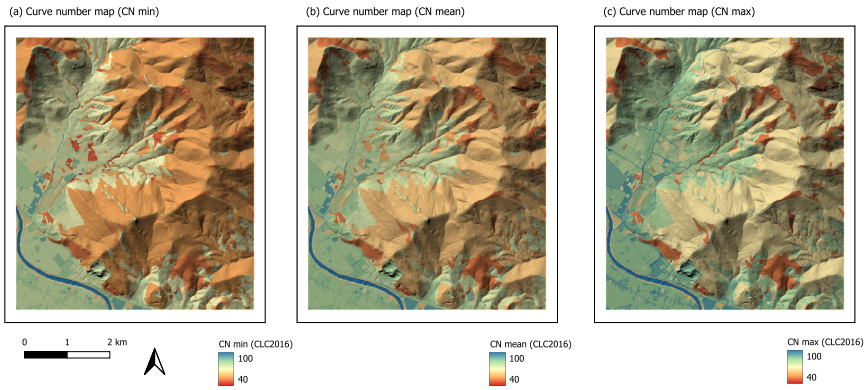

Figure 6: Curve number maps derived from combining a land use/land cover classes from Corine Land Cover 2016, hydrology conditions (hc) and Hydrologic Soil Group (HSG).

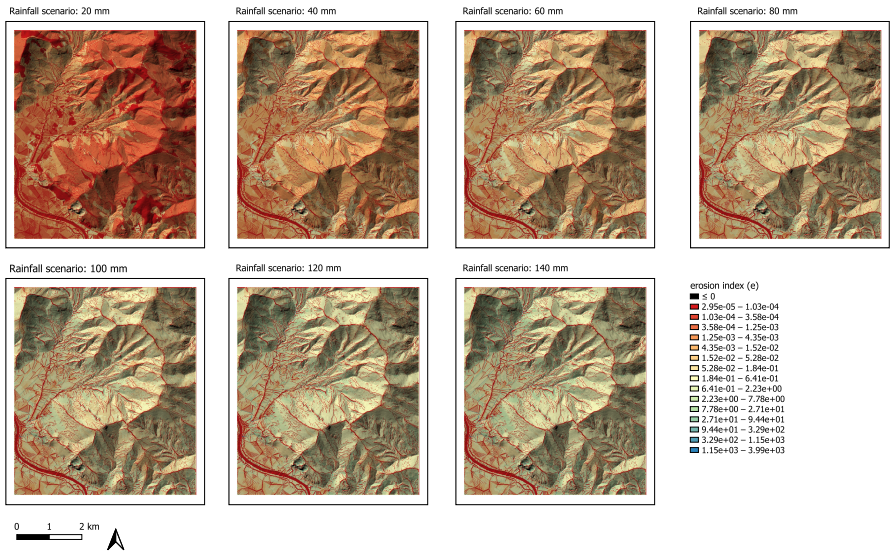

Figure 7: Results of `LANDPLANER` simulations in terms of erosion index (e) for different synthetic rainfall scenarios, considering CN map derived from CLC2016 (pre-fire event).

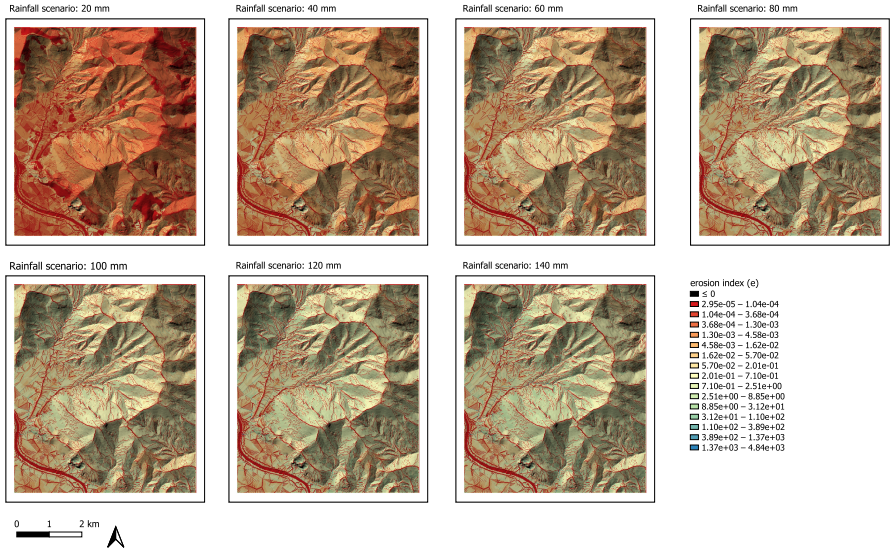

Figure 8: Results of `LANDPLANER` simulations in terms of erosion index (e) for different synthetic rainfall scenarios, considering CN map derived from CLC2019 (post-fire event).

4.4 Injecting vegetation

The vegetation map, represented in Figure 10, is used as a ground truth. Operatively, it is sampled by different configuration, to generate synthetic sampling pattern to validate the stochastic procedure prior to introduce in erosion modelling. Results of this validation procedure are in-depth described in Section 5.

Considering the synthetic sampling scheme with a regular pattern 100×100 m covering the DTM delimited area, samples (i.e., a triplet of georeferenced coordinates and an associated vegetation class) are processed from a geostatistical point of view. Samples are converted by the indicator encoding (Equation (1)) and a geostatistical directional analysis (Equation (2)) is performed in the 2D space following the approach described in Section 3.

In this case, geostatistical analysis means computing indicator variogram for each vegetation class. For simplicity, a unique correspondence between vegetation description classes and an integer identifier is created. (i.e., *1–castanea, 2–altre latifoglie, 3–macchia a leccio, 4–macchia a sughera, 5–bosco misto di pino e castagno, 6–pineta, 7–formazione di pino post incendio, 8–formazione di macchia post incendio, 9–agricolo/altre superfici non boscate*).

Exploiting the computed variography, the Sequential Indicator Simulation (SIS) algorithm is performed on punctual observations of vegetation according to the selected sampling schemes. Results are represented as spa-

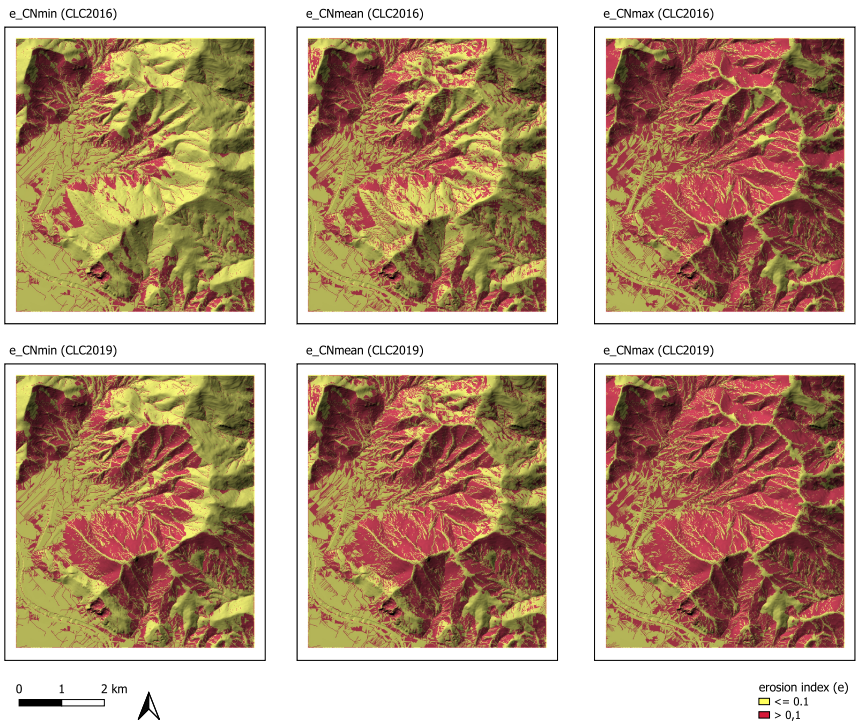

Figure 9: Pre- and post- fire event comparison between erosion maps computed by (a) minimum, (b) average and (c) maximum Curve Number distribution maps.

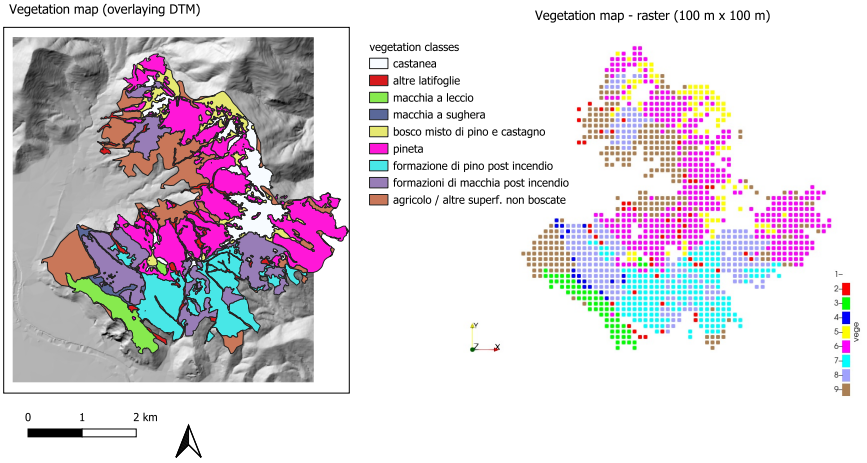

Figure 10: (a) Vegetation map (derived from [BST+04]) overlaying DTM (in shaded relief representation) of the Monte Pisano site, composed of n. 9 vegetation classes detected in pre-fire event (August, 2018). (b) A synthetic sampling configuration derived from vegetation map (resolution of 100 m $\times$ 100 m).

tial distribution maps of vegetation categories on a regular grid-based mesh representation (10×10 m). The figure 11 shows the results in terms of best guess obtained respectively for the three sampling configurations, (a) random, (b) regular 100×100 m, (c) regular 200×200 m. Each pixel contains the probability of occurrence of each considered category: the best scenario is obtained by finding the highest probability value for each cell. The entire computation is performed by a self-contained, stochastic-based tool (`MUSE` [Mio25, MCPVZ22]).

The spatial maps, previously generated, are combined to correct the Curve Number distribution map, explicitly accounting the hydrologic condition parameter h_c.

Firstly, an empirical eco-hydrologic coefficient of α_{cat} is assigned to each category, hydrological effectiveness of vegetation classes in terms of interception, soil protection, and infiltration. Higher values were associated with mature and structurally complex communities, such as holm oak maquis ($\alpha_{cat} = 0.95$) and chestnut or mixed forests ($\alpha_{cat} \approx 0.90$), while intermediate values were assigned to broadleaf formations ($\alpha_{cat} = 0.80$) and pine forests ($\alpha_{cat} = 0.75$), reflecting more heterogeneous or secondary conditions. Post-fire formations were assigned markedly lower values ($\alpha_{cat} = 0.25$–0.35) to account for reduced cover and increased runoff, whereas agricultural and non-forested areas were set to $\alpha_{cat} = 0.50$. This parameterization captures the main disturbance-driven eco-hydrological gradients of the study area.

ID	Category name	α_{cat}
1	Chestnut (*Castanea*)	0.90
2	Other broadleaf trees (*Altre latifoglie*)	0.80
3	Holm oak scrub (*Macchia a leccio*)	0.95
4	Cork oak scrub (*Macchia a sughera*)	0.80
5	Mixed pine and chestnut (*Bosco misto di pino e castagno*)	0.90
6	Pine forest (*Pineta*)	0.75
7	Post-fire pine stand (*Formazione di pino post-incendio*)	0.35
8	Post-fire scrubland (*Formazioni di macchia post-incendio*)	0.25
9	Agricultural / other non-forested areas (*Agricolo / altre superfici non boscate*)	0.50

Table 2: Empirical values of α_{cat} coefficient for each vegetation classes, labelled by a unique identifier (ID) and a descriptive name.

The assigned values are indicated in the Table 2.

Then, an alpha-coefficient map is generated by combining α_{cat} with the probability of occurrence of each category $P_{cat}(x)$ obtained by SIS algorithm (Equation (3)).

$$\alpha(x) = \sum P_{cat}(x) * \alpha_{cat} \tag{3}$$

with $cat = (1, \ldots, 9)$ representing all vegetation classes mapped in Figure 10.

Finally, the α–map is used to correct the CN distribution map, according to the Equation (4).

$$CN_{corr}(x) = CN_{poor}(x) + \alpha(x) * (CN_{good}(x) - CN_{poor}(x)) \tag{4}$$

In this way, we produce a new corrected CN map, accounting for sub-grid vegetation variability, to be used replacing the deterministic-oriented CN map.

5 Results and discussion

The section describes the results obtained for the application of the enhanced hydrological framework on the Monte Pisano site. The contribution is twofold: firstly, we test the stochastic approach on vegetation classes, validating the method (Section 5.1); secondly, we correct CN with stochastic map of vegetation, evaluating the impact on erosion assessment (Section 5.2).

5.1 Validating stochastic on vegetation classes

Prior to involving the stochastic approach on the hydrogeological framework, we validate the robustness of the stochastic-based approach across datasets with varying sampling schemes (e.g., regular grids vs random sampling) and

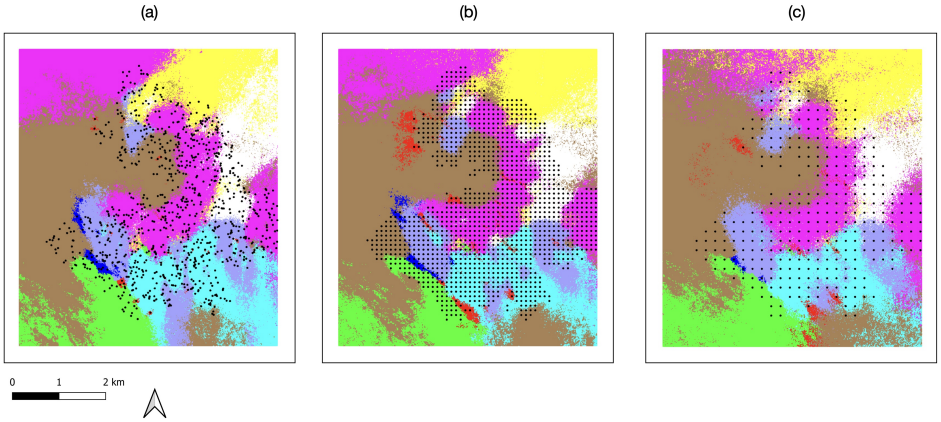

Figure 11: Visual comparison of sequential indicator simulation (best guess) on regular grid mesh support (10×10 m) for three different synthetic sampling scenario used for validation: (a) random, (b) regular 100×100 m, and (b) regular 200×200 m.

spatial resolutions. For each configuration, multiple stochastic realizations are generated and compared in terms of predictive performance and spatial agreements.

Figure 11 shows the results in term of the best guess for the three selected sampling configurations, respectively: (a) random sampling, (b) regular sampling with 100×100 meters of spacing, (c) regular sampling with 200×200 meters of spacing.

Comparing SIS-results and the ground truth (Figure 10), results highlight the strong influence of sampling design on classification performance, as well as the importance of ensuring spatial consistency in the validation procedure. Among the tested configurations, the regular grid with 100×100 m spacing consistently achieves the highest *overall accuracy* and *Cohen's Kappa* coefficient [Coh60], indicating that an intermediate sampling resolution provides the best compromise between spatial representativeness and coverage. In contrast, the coarser 200×200 m grid leads to a systematic decrease in performance, suggesting that excessively sparse sampling fails to capture fine-scale heterogeneity in vegetation patterns. The random configuration yields intermediate results, likely reflecting its irregular spatial distribution, which may result in locally clustered or undersampled areas.

A key outcome of this study is the substantial difference observed between filtered and unfiltered accuracy assessments. When all simulated points are considered, including those outside the spatial extent of the ground truth, overall accuracy is significantly underestimated. Restricting the evaluation to points falling within the ground truth polygons results in a marked increase in both metrics across all configurations. This discrep-

Table 3: Overall accuracy (OA) and Cohen's kappa (K) for the three sampling configurations.

	areas dismatch		*overalapping areas*	
Configuration	OA	K	OA	K
Random	0.6217	0.5522	0.7305	0.6741
Grid 100x100	0.6534	0.5875	0.7637	0.7152
Grid 200x200	0.5781	0.4983	0.6881	0.6229

ancy reveals a methodological bias introduced by evaluating geostatistical predictions outside the reference domain, where no input data exist. These findings emphasize the necessity of spatial alignment between prediction and validation datasets to ensure reliable performance estimates.

The entropy-based metric reliably captures model uncertainty, with higher entropy correlating with lower maximum class probabilities and misclassifications. Spatially, high-entropy areas align with class boundaries and heterogeneous zones, while finer 100×100 m grids reduce the extent of uncertain regions, highlighting the influence of sampling design. Distinguishing validation and prediction domains allows accurate assessment and full-area mapping, which is crucial for applications like erosion modelling. Overall, combining careful sampling, validation, and uncertainty analysis ensures robust spatial predictions and informs interpretation of less reliable areas. These aspects are showed in Figure 12.

5.2 Erosion modelling

To extend the geostatistical vegetation modelling framework to hydrological applications, the simulated vegetation classes were used to correct the Curve Number (CN) map, as described in Section 4.4. Figure 13 shows the erosion index map computed by `LANDPLANER` and employing the corrected CN map.

Beyond a deterministic assignment based on the most probable class, a probabilistic approach was adopted to account for classification uncertainty, computing CN values as the expected value derived from class probabilities. This approach allows for a smoother and more realistic spatial representation of hydrological response, particularly in heterogeneous or transitional areas.

A series of metrics are selected to quantify the effectiveness of results. Comparison with the deterministic estimates shows that the stochastic framework introduces localized, probabilistically guided adjustments while preserving overall spatial structure. Mean erosion slightly decreases, with a moderate reduction in variability, indicating a smoothing of extreme values while preserving the general distribution. Agreement metrics confirm the strong consistency between the two maps (e.g., *Pearson correlation coefficient* $r = 0.998$; *Nash-Sutcliffe Efficiency parameter* $NSE = 0.995$).

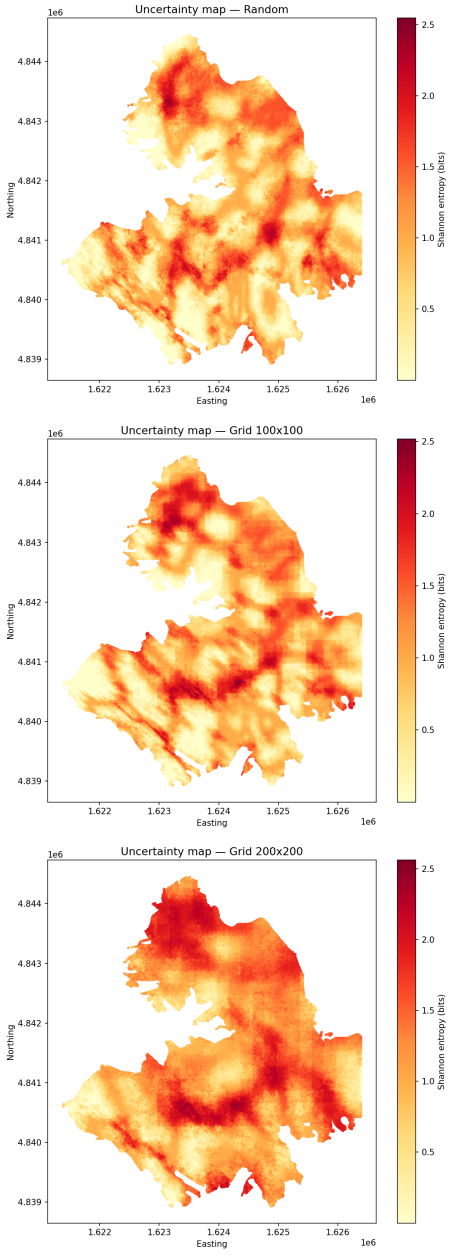

Figure 12: Entropy plots obtained for three sampling configurations.

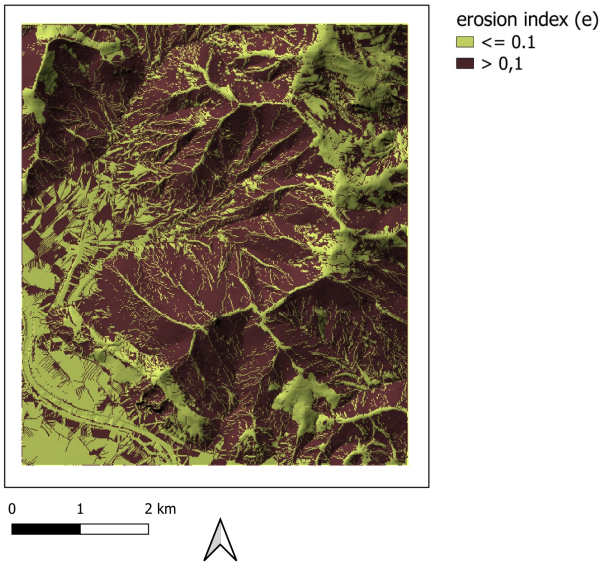

Figure 13: Pre-fire event erosion index map, simulated for a synthetic rainfall scenario of 120 mm and computed by the corrected Curve Number distribution map.

Spatially, the correction produces both increases and decreases at the pixel scale, while slightly moderating the highest erosion values.

Overall, the stochastic approach integrates vegetation-driven sub-grid variability and associated uncertainty while maintaining spatial coherence with deterministic patterns, resulting in a more robust and interpretable erosion representation.

6 Limitations and future works

A key limitation of the current work is the use of an empirical value of α_{cat} for modulating the probability. An improvement of the method could be considered real information about the vegetation behaviour and used these to combine the class probability.

Future work will explore the integration of the geostatistical spatialization techniques with geotechnical soil parameters for infiltration models. Additionally, extending the approach to incorporate spatially distributed rainfall inputs, rather than synthetic ones, could further enhance model realism and predictive capability.

To enhance the impact of the methodology, an interesting future work is to consider temporal vegetation evolution, seasonal effects or post-fire recovery, expanding the application across time.

7 Conclusion

The paper proposes a computational framework for incorporating vegetation spatial variability into erosion modeling through indicator-based geostatistical simulation coupled with Curve Number (CN) estimation for runoff and erosion prediction. The effectiveness of the combined approach is demonstrated on a post-wildfire real case study in Monte Pisano (Tuscany, Italy). The work aims to bridge the gap between traditional simplified operational models and computationally intensive coupled biogeomorphic models, offering a practical pathway for uncertainty-aware erosion assessment.

Validation shows that the stochastic vegetation model produces results broadly consistent with deterministic approaches while providing added value through the quantification of uncertainty. The entropy-based metric effectively identifies areas of high model uncertainty, which are concentrated along class boundaries and heterogeneous zones, and highlights regions where predictions are less reliable. Finer grid configurations (e.g., 100×100m) reduce the spatial extent of high-uncertainty areas, illustrating the importance of sampling design in both classification accuracy and the spatial distribution of uncertainty. Distinguishing between validation and prediction domains allows reliable accuracy assessment and the generation of spatially continuous vegetation maps, which are essential for downstream applications such as runoff estimation and erosion modelling.

Overall, this approach supports more informed decision-making by providing both spatially explicit predictions and associated confidence measures, representing a meaningful step forward in integrating biodiversity and hydro-geomorphological modelling.

8 Acknowledgments

This research is funded under the National Recovery and Resilience Plan (NRRP), Mission 4 Component 2 Investment 1.4 - Call for tender no. 3138 of 16 December 2021, rectified by Decree no. 3175 of 18 December 2021 of Italian Ministry of University and Research funded by the European Union-NextGenerationEU; Award Number: Project code CN 00000033, Concession Decree no. 1034 of 17 June 2022 adopted by the Italian Ministry of University and Research, CUP B83C22002930006, Project title “National Biodiversity Future Center - NBFC”.

The authors would like to acknowledge Simone Pittaluga for the Sequential Indicator Simulations algorithm implementation supporting stochastic computation on mesh.

References

[AMTR22] Margherita Agostini, Alessandro Cesare Mondini, Dino Torri, and Mauro Rossi. Modelling seasonal variation of gully erosion at the catchment scale. *Earth Surface Processes and Landforms*, 47(2):436–458, 2022.

[BST+04] Andrea Bertacchi, Alessandra Sani, Paolo Emilio Tomei, et al. *La vegetazione del Monte Pisano*. Felici Pisa, Italy, 2004.

[CCCP13] Luigi Carmignani, Paolo Conti, Gianluca Cornamusini, and Altair Pirro. Geological map of tuscany (italy). *Journal of Maps*, 9(4):487–497, 2013.

[Coh60] Jacob Cohen. A coefficient of agreement for nominal scales. *Educational and psychological measurement*, 20(1):37–46, 1960.

[CPA+24] Dov Corenblit, Hervé Piégay, Florent Arrignon, Eduardo González-Sargas, Anne Bonis, Dav M. Ebengo, Virginia Garófano-Gómez, Angela M. Gurnell, Annie L. Henry, Borbála Hortobágyi, Francisco Martínez-Capel, Lucas Mazal, Johannes Steiger, Eric Tabacchi, Stephen Tooth, Franck Vautier, and Romain Walcker. Interactions between vegetation and river morphodynamics. Part II: Why is a functional trait framework important? *Earth-Science Reviews*, 253:104709, 2024.

[Del87] Studio geomorfologico della pianura di pisa: Geomorphology of the pisa plain (tuscany). 10:56–84, Jun. 1987.

[Ehl89] CR Ehlschlaeger. Using the Aˆ T search algorithm to develop hydrologic models from digital elevation data. In *Proceedings of the international geographic information system (IGIS) symposium, Baltimore, MD*, pages 275–281, 1989.

[EL09] Jane Elith and John R Leathwick. Species distribution models: ecological explanation and prediction across space and time. *Annual review of ecology, evolution, and systematics*, 40(1):677–697, 2009.

[Fra45] Janet Franklin. Mapping species distributions. *American history*, 1861(1900), 1945.

[G+97] Pierre Goovaerts et al. *Geostatistics for natural resources evaluation*. Oxford University Press on Demand, 1997.

[GG16] Stefano Luigi Gariano and Fausto Guzzetti. Landslides in a changing climate. *Earth-Science Reviews*, 162:227–252, 2016.

[GU04] ML Gandini and EJ Usunoff. Curve number estimation using remote sensing ndvi in a gis environment. *Journal of environmental hydrology*, 12, 2004.

[Gur14] Angela Gurnell. Plants as river system engineers. *Earth Surface Processes and Landforms*, 39(1):4–25, 2014.

[Hau11] Natalie Haussmann. Biogeomorphology: Understanding different research approaches. *Earth Surface Processes and Landforms*, 36:136 – 138, 01 2011.

[HWWVM08] Richard H Hawkins, Timothy J Ward, Donald E Woodward, and Joseph A Van Mullem. Curve number hydrology: State of the practice. American Society of Civil Engineers, 2008.

[Mar10] Richard A. Marston. Geomorphology and vegetation on hillslopes: Interactions, dependencies, and feedback loops. *Geomorphology*, 116(3):206–217, 2010. Geomorphology and Vegetation: Interactions, Dependencies, and Feedback Loops.

[MCPVZ22] Marianna Miola, Daniela Cabiddu, Simone Pittaluga, and Marino Vetuschi Zuccolini. MUSE: Modeling Uncertainty as a Support for Environment. In Daniela Cabiddu, Teseo Schneider, Dario Allegra, Chiara Eva Catalano, Gianmarco Cherchi, and Riccardo Scateni, editors, *Smart Tools and Applications in Graphics - Eurographics Italian Chapter Conference*. The Eurographics Association, 2022.

[MHHJ19] Muluken E. Muche, Stacy L. Hutchinson, J.M. Shawn Hutchinson, and John M. Johnston. Phenology-adjusted dynamic curve number for improved hydrologic modeling. *Journal of Environmental Management*, 235:403–413, 2019.

[Mio25] Marianna Miola. *Increase the knowledge of Natural Systems through the evaluation of the uncertainty of environmental data: operational theory and application*. PhD thesis, Università degli Studi di Genova, 2025.

[MS03] Surendra Kumar Mishra and Vijay P Singh. Scs-cn method. In *Soil conservation service curve number (SCS-CN) methodology*, pages 84–146. Springer, 2003.

[R+91] FosterGR RenardKG et al. RUSLE: Revised Universal Soil Loss Equation. *JournalofSoilandwaterConser vation*, 46(1):30, 1991.

[Ren97] Kenneth G Renard. *Predicting soil erosion by water: a guide to conservation planning with the Revised Universal Soil Loss Equation (RUSLE)*. US Department of Agriculture, Agricultural Research Service, 1997.

[Ros14] Mauro Rossi. *Modelling of landslide phenomena and erosion processes triggered by meteo-climatic factors*. PhD thesis, Università degli Studi di Perugia, Dipartimento di Fisica e Geologia, 2014.

[RT74] Antonio Rau and Marco Tongiorgi. Geologia dei Monti Pisani a Sud-Est della Valle del Guappero. 1974.

[SFAB20] Fabio Salbitano, Cristiano Foderi, and Andrea Andrea Bertacchi. Documento tecnico per il ripristino dei soprassuoli forestali del monte pisano. Technical report, Direzione Agricoltura e Sviluppo Rurale. Regione Toscana, 2020.

[SVDL09] KX Soulis, JD Valiantzas, N Dercas, and PA Londra. Investigation of the direct runoff generation mechanism for the analysis of the scs-cn method applicability to a partial area experimental watershed. *Hydrology and Earth System Sciences*, 13(5):605–615, 2009.

[TP14] Dino Torri and Jean Poesen. A review of topographic threshold conditions for gully head development in different environments. *Earth-science reviews*, 130:73–85, 2014.

[usd21] Technical report, 2021.

[Vil20] Heather Viles. Biogeomorphology: Past, present and future. *Geomorphology*, 366:106809, 2020.

[VNN11] Peter H Verburg, Kathleen Neumann, and Linda Nol. Challenges in using land use and land cover data for global change studies. *Global change biology*, 17(2):974–989, 2011.

[WS78] Walter H Wischmeier and Dwight David Smith. *Predicting rainfall erosion losses: a guide to conservation planning*. Number 537. Department of Agriculture, Science and Education Administration, 1978.

[WZS+25] Miaomiao Wang, Yangdong Zhao, Wenhai Shi, Jinle Yu, Tiantian Chen, Jiachi Bao, Wenyi Song, and Hongjun Chen. A modified curve number method for runoff prediction of different soil types in china. *CATENA*, 254:108957, 2025.

[YCW+25] Jinle Yu, Hongjun Chen, Miaomiao Wang, Jiachi Bao, Wenyi Song, Xitong He, and Wenhai Shi. A modified curve number method for runoff prediction of different vegetation types at the slope scale in China. *Soil and Tillage Research*, 254:106737, 2025.